JOURNAL OF PROPULSION AND POWER
Vol. 12, No. 2, March–April 1996

Performance Characterization of a Highly Offset Diffuser with Vortex Generator Jets

M. B. Senseney,* T. A. Buter,† and R. D. W. Bowersox‡
U.S. Air Force Institute of Technology, Wright–Patterson Air Force Base, Ohio 45433

The effect of blowing vortex generator jets on the performance of a highly offset (S-duct) diffuser was investigated experimentally ($M_1 = 0.6$, $Re_{eq} = 3.46 \times 10^7$). Inlet plane total pressure and Mach number contours were mapped using a pitot probe. Exit plane total pressure recovery, static pressure recovery, and Mach number contours were mapped with blowing on and off, using pitot and static probes. Cross-wire anemometry was used to measure the mean velocity and turbulence intensity in three dimensions at three spanwise locations on the exit plane with the blowing on and off. Without blowing, the flow on the lower surface of the diffuser was massively separated. Blowing at 0.50% mass flow ratio through three lower-surface vortex generator jets reduced the size of the separated-flow region and the exit plane boundary-layer thickness, increased pressure recovery, and decreased turbulence intensity. Blowing redistributed momentum within the diffuser and altered the secondary flow structure. However, the exit plane total and static pressure fields were more distorted with blowing than without.

Nomenclature

A = area
b = diffuser span
C_p = pressure coefficient
L = diffuser length
M = Mach number
$\dot{m}$ = mass flow rate
P = pressure
Re_δ = Reynolds number, $U_\infty \delta / \nu_\infty$
T = temperature
U_∞ = freestream velocity
u, v, w = velocity components in Cartesian frame
x, y, z = Cartesian coordinates

Subscripts

e = exit
eq = equivalent
i = inlet
j = jet
ref = reference
s = static
$t, 0$ = total
δ = boundary-layer thickness
∞ = freestream

Superscripts

$'$ = fluctuating quantity
$\bar{}$ = mean quantity

Introduction

JET engine inlet diffuser design has become an increasingly important element in the optimization of overall aircraft propulsion system performance. Along its length the diffuser reduces the velocity of the air and increases its static pressure. Ideally, the diffuser would convert all of the kinetic energy removed from the air to pressure energy. However, losses occur because of the dissipative action of viscosity. Characteristically, flow in a diffuser is subjected to an adverse axial pressure gradient. This adverse pressure gradient enhances boundary-layer growth and promotes separation. A thick or separated boundary layer in the diffuser typically produces large regions with reduced axial velocity, increased transverse velocities, and increased turbulence at the engine face. The energy lost through these flow processes is manifested by a reduction in total pressure in the diffuser.

Frequently, it is advantageous to bury the engines into the aircraft structure. The diffuser is then tasked with the additional requirement of turning the air as well as decelerating it and increasing its static pressure. Further, constraints on system weight and volume often require the diffuser to do all of this in as short a length as possible. These considerations have led to the development of short (and, therefore, highly divergent), highly offset (S-duct) diffusers. The advantages of this type of diffuser may be exploited by civil transport aircraft, where the weight and volume savings can increase operating revenues; and by military combat aircraft, where reduced infrared, radar, and acoustic signatures are also desired. Some examples of aircraft using S-duct diffusers are the Boeing 727 and Lockheed L-1011 transports, and the Northrop B-2, McDonnell Douglas F-18, and the Lockheed Martin F-22 military aircraft. Unfortunately, the gains in structural efficiency, weight reduction, and signature reduction achieved with short, highly offset diffusers must be traded off against the reduced efficiency of these diffusers. Reducing the length of a diffuser induces an increase in the adverse axial pressure gradient to achieve equivalent diffusion. A transverse pressure gradient forms because of the curvature of the duct in the streamwise direction, creating a secondary flow that in turn draws low momentum boundary-layer fluid from the perimeter towards the inner convex surface. These factors promote boundary-layer growth and increase the likelihood of separation. A short, highly offset diffuser is likely to have substantially poorer pressure recovery, higher levels of turbulence, and increased distortion at its exit plane than a straight-walled diffuser. Increased levels of turbulence and distortion affect the structural integrity of the compressor as well as impacting performance. Thus, the effects of the flow peculiarities found in S-duct dif-

Received May 1, 1995; revision received Oct. 20, 1995; accepted for publication Oct. 31, 1995. This paper is declared a work of the U.S. Government and is not subject to copyright protection in the United States.

*Graduate Research Assistant, Department of Aeronautics and Astronautics. Member AIAA.

†Assistant Professor, Department of Aeronautics and Astronautics. Senior Member AIAA.

‡Assistant Professor, Department of Aeronautics and Astronautics. Member AIAA.

fusers are significant enough to warrant consideration and attempts at control.

Three main techniques are commonly employed to minimize the dissipative effects of viscosity as a fluid flows over a body or through a duct. One approach seeks to control the boundary layer by re-energizing it with a small mass of high-momentum fluid blown through slots or jets in the wall boundary. Another removes the low-momentum boundary layer, or at least retards its growth, by using suction to draw fluid through slots or a porous surface. Both of these types of boundary control are called active methods. Finally, passive devices such as vortex generators diminish boundary-layer growth and discourage separation by enhancing the mixing of high-momentum fluid from the freestream with low-momentum fluid in the boundary layer. All of these methods have been tested extensively in straight or nearly straight walled diffusers. Adkins[1] provides a summary of the relative effectiveness of several boundary-layer control (BLC) schemes when applied to several conventional types of diffusers. The current study combines aspects of two of these approaches: 1) blowing and 2) the promotion of mixing associated with vortex generators, as a means for improving diffuser performance.

A study of seven different blowing schemes by Ball[2] showed that a combination of discrete blowing holes and solid vortex generators produced the best results, providing a total pressure recovery increase of approximately 1.0% with a blowing mass flow of only 0.4% of diffuser inlet mass flow, suggesting that some combination of high-momentum fluid injection and vortex generation may provide a relatively efficient means for improving diffuser performance. Vortex generator jets (VGJ) represent just such a combination.

Wallis[3] first showed that a pitched, skewed blowing jet generates a streamwise vortex as it adds high-momentum fluid to the flow. Johnston and Nishi[4] dubbed this type of jet a VGJ. They verified the existence of these vortices in a very low-speed flow (U_{ref} = 15 m/s) and showed that these vortices are sufficiently strong, under the proper circumstances, to substantially reduce and nearly eliminate a large stalled region of turbulent separated flow over a flat plate.

Selby et al.[5] performed a parametric investigation to find the optimum combination of vortex generator jet geometric and flow properties to control separation on an aft-facing ramp in low-speed (U_{ref} = 40 m/s) airflow. Selby found the optimum inclination (pitch) angle to be between 15–20 deg relative to the local surface tangent, the optimum skew angle to be between 60–90 deg relative to the nominal flow axis, and the optimum jet diameter to be as small as possible, to maximize the jet-to-freestream velocity ratio. Selby also found that VGJs retained significant separation-control effectiveness when located up to 40 boundary-layer thicknesses upstream of the baseline (no blowing) separation point, but were most effective when located just upstream of the baseline separation point. Finally, the study showed that a spanwise array of jets skewed in the same direction to produce corotating vortices was more effective than an array of jets oriented to produce counter-rotating vortices. Lin et al.[6] performed a study comparing the performance of several passive and active methods for controlling separation on a similar aft-facing ramp, and found VGJs to be one of the most effective methods.

While the vortex generator jet concept has been studied for a variety of external, incompressible, two-dimensional flows, investigations that consider diffuser-like configurations are scarce. The primary objective of the current study was to evaluate the effect of vortex generator jets on the total pressure recovery, coefficient of pressure, and turbulent structure of the flow at the exit plane of a representatively short, highly offset diffuser. A secondary objective was to provide data suitable for use as a validation case for computational fluid dynamic (CFD) models of geometrically similar diffuser designs.

Experimental Procedure

Tests were conducted on a subscale rectangular cross-sectional diffuser at an inlet Mach number of 0.6. Ball[7] found that data from a rectangular cross-sectional diffuser demonstrated the same general trends as that from a more representative round cross-sectional duct, and so it was deemed suitable for the investigative nature of this study.

Model Specifications

A schematic of the diffuser test section is provided in Fig. 1. The diffuser inlet was sized to allow continuous operation at M_i = 0.8 when connected to the facility pressurized air supply. The diffuser inlet plane dimensions were 2.54 × 1.679 cm. Achieving typical engine inlet diffuser exit conditions of M_e = 0.4–0.5 required an area ratio of approximately (A_e/A_i) = 1.5; the exit plane dimensions were then fixed at 2.54 × 2.54 cm. The equivalent diameter D_{eq} of the exit plane, defined as the diameter of a circle with an equivalent cross-sectional area, was 2.882 cm. The test rig was operated at 0.52 MPa gauge supply pressure with an airflow of 0.45 kg/s to obtain the desired inlet Mach number condition of M_i = 0.6.

The values of the two other parameters that defined the geometry of the test section correspond to those of a highly offset diffuser tested extensively by McDonnell Aircraft Company as part of the U.S. Air Force Wright Aeronautical Laboratories Subsonic Diffusers for Highly Survivable Aircraft program.[8] Two other geometric parameters were needed to define the diffuser. The length parameter, which specifies the axial distance over which the diffusion is to occur was set to L/D_{eq} = 2.07. Along with the area ratio, this establishes the axial pressure gradient. The centerline offset parameter is an indirect measure of duct curvature and was set to $(\Delta y/D_{eq})$ = 0.81. The cross-sectional area of the test diffuser increased linearly from the beginning of the divergence until the exit area was achieved. The centerline curvature was determined by a third-order curve fit:

$$y = 0.22050x^3 - 0.197365x^2 + 0.000982x - 0.8395 \quad (1)$$

where x and y are in centimeters.

The test section was machined from aluminum, and Plexiglas® sidewalls installed to facilitate flow visualization (Fig. 1). A spanwise array of three vortex generator jets was installed in the lower surface. The jets were constructed by drilling oversized pitched and skewed holes into the flow-path surface, then inserting 0.0572-cm-i.d. thin-walled tubing through the holes. The jet exit plane was located 1.27 cm downstream of the beginning of the curved, diffusing passage. The jets were canted 45 deg in the direction of decreasing z, so that they blew toward the left sidewall when looking downstream and were pitched 25 deg relative to the lower surface tangent. The jet orientation was based on the results of Selby et al.,[5] though the optimum cant angle could not be attained because of manufacturing limitations.

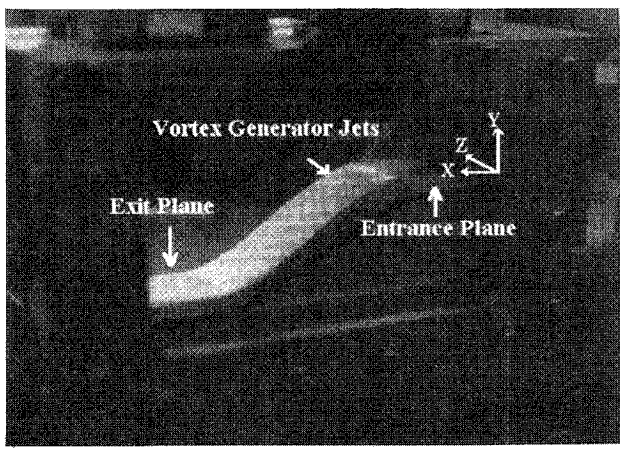

Fig. 1 Diffuser test section.

Table 1 Uncertainty analysis summary

Measured quantity	Estimated error, %
Total pressure	±1.5
Static pressure	±1.0
Surface static pressure	±1.0
Hot-film velocity	±6.3

Data Acquisition

To obtain inlet measurements out of the influence of the duct curvature, and to allow the probes to reach as much of the cross section as possible, the inlet plane was defined in the straight, constant area portion of the test section 1.65 cm upstream of the beginning of the divergence and curvature (Fig. 1). The diffuser exit plane was defined as the axial station where curvature and divergence ended and the test section flow path resumed a straight, constant-area cross section. The distance between the inlet and exit planes was 7.66 cm.

Six static pressure ports in the lower surface allowed measurement of the axial pressure distribution. Pitot pressure, static pressure, and hot-film probes were inserted through the upper surface to measure flow properties across the inlet and exit planes. The separate pitot and static pressure rakes were constructed from 0.14732-cm-o.d. thin-walled tubing bent to an L-shape. The edges around the orifice of the pitot probe were beveled, thereby presenting less of a blunt edge to the oncoming flow. The closed end of the static probe upstream of the four diametrically opposed sensing ports was rounded to prevent flow separation. Total pressure information was obtained at the inlet and exit planes with and without blowing at $M_i = 0.6$. Pitot data were collected every 0.254 cm across the span. The static pressure measurements were spaced 0.508 cm apart. Data in the y direction was spaced every 0.794 mm. Lower surface static pressure data were taken during these runs as well. All pressure measurements were sampled for 1 s at 50 Hz.

Blowing-on and blowing-off cross-film probe data were obtained at three spanwise locations along the exit plane. Sweeps began at $y = 0.153$ cm above the test section floor and continued in 0.794-mm increments for 15 steps. Hot-film signals were sampled at 100 KHz for 0.2 s at each measurement station. The pitot pressure, static pressure, and hot-film probes traversed in the y direction under the control of a personal-computer-based robotic system. Probes were manually positioned to the desired z position for each run.

Surface flow visualization was performed by placing thin lines of an oil-based dye on the internal surfaces of the test section. Results were documented through sketches, still photographs, and video footage and used to ensure that the blowing ports were installed upstream of the separation line. Unfortunately, the poor reproductive quality of the photographs prevented their inclusion in this article.

Uncertainty Analysis

The results of a detailed uncertainty analysis[9] are summarized in Table 1. This analysis showed that the largest error components were because of probe placement uncertainty ($x \pm 0.036$ cm and $y \pm 0.071$ cm). Total pressure and hot-film velocity measurements were very sensitive to position as significant velocity and pressure gradients existed in the measurement planes. The effect of random errors was essentially eliminated by the large number of samples that comprised each data point.

Results and Discussion

From the data obtained during this study, it was possible to characterize the performance of the test diffuser for blowing-off and one blowing-on case at $M_i = 0.6$, and to gain some insight about the flow processes that drove the performance. Some data was collected at $M_i = 0.8$, but problems with hot-film durability precluded collection of a complete data set. The results are divided into two categories: 1) mean flow properties, the overall, time-averaged behavior of the fluid that determines the bulk measures of performance such as pressure coefficient, pressure recovery, and efficiency; and 2) turbulent flow properties, which help understand the flow processes and the performance by quantifying the amount of energy that is lost to random motion.

Inlet Flow Properties

Figure 2 shows a map of the total pressure recovery at the diffuser inlet plane for $M_i = 0.6$. While there was a large region in the center of the cross section where the flow was relatively undisturbed from freestream conditions, the lower surface wall boundary layer was approximately 10% of the span of the test section.

One vertical sweep of the centerline at $M_i = 0.6$ showed that the static pressure varied by less than 3.46 KPa across the height of the test section. Based on this information, the pressure measured at the tap located on the lower surface centerline was taken as the value of the static pressure everywhere on the inlet plane. Mach number was calculated from measured values of P_t and P_s through isentropic flow relationships. The nominal $M_i = 0.6$ condition gave a maximum Mach number of 0.605. From run-to-run, the inlet plane Mach number was repeatable to within ±0.005.

Using the total temperature measured in the settling chamber, isentropic flow relationships, and the perfect gas law, velocity profiles were generated for the lower surface boundary layer at the centerline. The boundary-layer thickness at this location, $\delta_{99\%}$, is roughly 0.272 cm. Comparison with the four

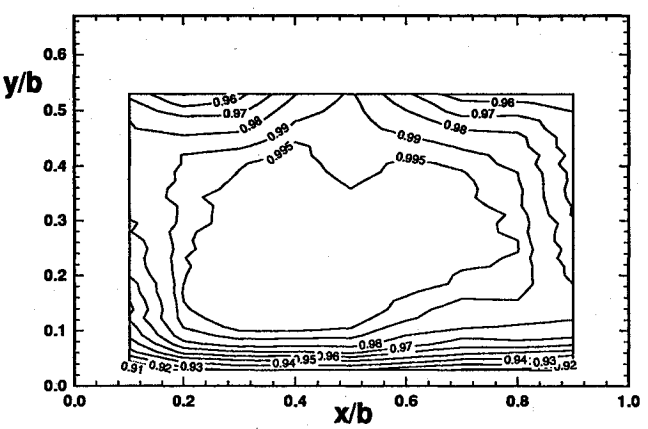

Fig. 2 Baseline inlet plane pressure recovery map.

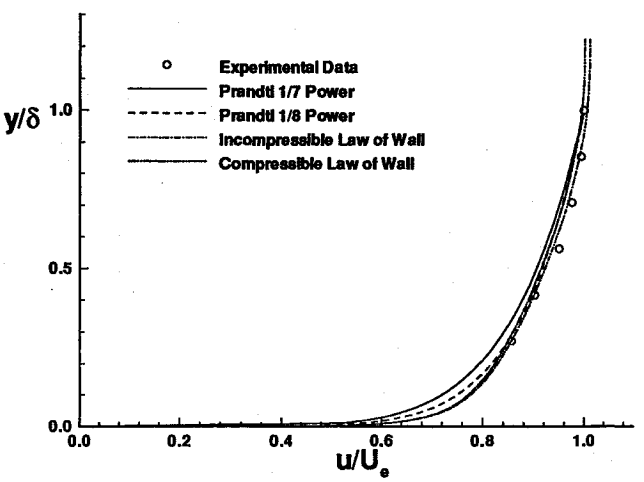

Fig. 3 Inlet plane boundary-layer profile, $M_i = 0.6$.

theoretical models for the turbulent boundary layer is presented in Fig. 3, the one-seventh power law, the one-eighth power law, the incompressible law-of-the-wall, and the compressible law-of-the-wall, indicated that the lower surface boundary layer at the inlet plane was turbulent. Because of the small size of the model, no data were collected in the boundary-layer's inner region. The one-eighth power law, recommended for high Reynolds number flows over the more common one-seventh power law, and either form of the law-of-the-wall, fit the data quite well. As can be seen, at $M_i = 0.6$, compressibility effects were small.

Exit Plane Properties

As a means of characterizing diffuser performance with and without vortex generator jets, a series of measurements were conducted at the exit plane of the diffuser (Fig. 1).

Total Pressure Measurements

Total pressure recovery is the performance measure most commonly used for aircraft engine inlet diffusers, since it quantifies the amount of energy lost during the diffusion process. As the pitot probe was aligned with the x axis, the measured total pressure was sensitive only to the $+u$ component of velocity. Spanwise and reverse flows could not be detected by the probe. The total pressure measured here then is a measure of the component of the fluid momentum directed along the axis of the diffuser. In practice, this is the component available to do useful work, for the energy contained in the other velocity components is not recovered unless the device to which the diffuser leads is specifically designed to use swirl.

Figure 4a shows the exit plane total pressure map without blowing. The blowing-off map clearly showed that a large amount of energy was lost in the separated lower-surface boundary layer. The face-averaged total pressure recovery, the area-weighted average of all the total pressure recovery measurements taken across the exit plane, was 0.93. This corresponded to an isentropic diffuser efficiency, as defined in Hill and Peterson,[10] of 0.69. The total pressure contour pattern was similar to that presented by Ball[7] for a rectangular cross-sectional highly offset diffuser.

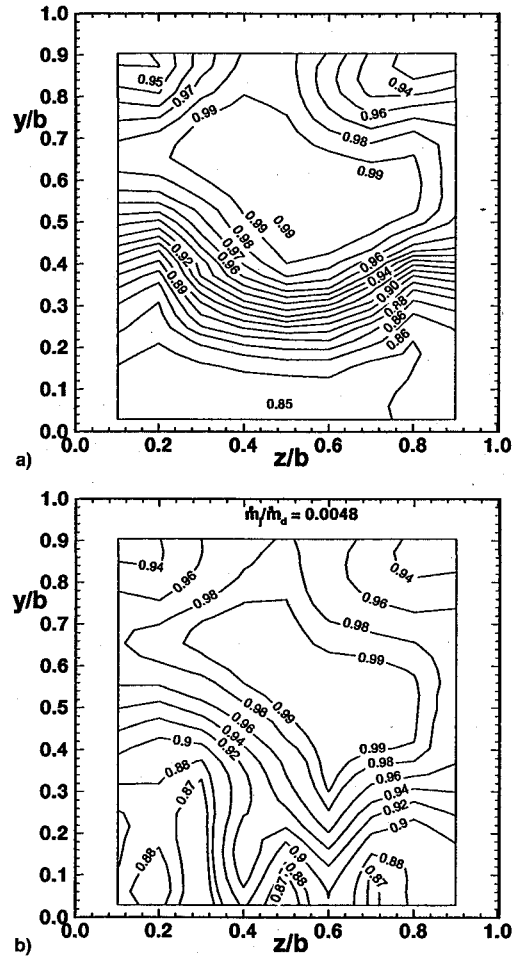

Fig. 4 Exit plane pressure recovery map: a) blowing off and b) blowing on.

Though it was depressed significantly from its freestream value, the total pressure field varied smoothly over the exit plane. The y component of the total pressure gradient in the lower half of the duct was quite uniform, and total pressure gradients in the z direction were significant only near the sidewalls and in the corner regions near the upper surface. Though most common methods of quantifying inlet distortion are not applicable to rectangular cross-sectional ducts, the distortion of the total pressure flowfield at the exit of the test diffuser was quantified in two ways. The maximum/minimum distortion method, defined $[(r_d|_{\max} - r_d|_{\min})/r_d|_{av}]$, measured the maximum variation of the total pressure recovery observed at any two points on the exit plane as a percentage of face-averaged value. The maximum gradient method, defined as $\{\max[\text{abs}(r_d|_{i\pm1,j} - r_d|_{i,j}, r_d|_{i,j\pm1} - r_d|_{i,j}]\}$, measured the maximum difference between the total pressure recovery methods taken at any two adjacent measurement stations. Without blowing, the values of distortion calculated by these methods were 0.170 and 0.06, respectively.

Compared to values measured without blowing, blowing at $(\dot{m}_j/\dot{m}_d) = 0.0048$ increased the pressure recovery on the right side of the diffuser quite substantially, but an accumulation of low-momentum fluid near the left sidewall actually reduced the total pressure recovery at some locations on that side of the diffuser (Fig. 4).

The lowest pressure recovery values were measured near the lower surface at $z/b = 0.3$, 0.5, and 0.7, directly downstream from the jet locations. Between those stations, the near-surface pressure recovery was increased nearly 5% over the blowing-off values. In the upper half of the exit plane, the total pressure contours appear nearly unchanged from the blowing-off case.

The overall face-averaged total pressure recovery for blowing at $(\dot{m}_j/\dot{m}_d) = 0.0048$ was 0.94, and the isentropic diffuser efficiency was 0.75. The min/max distortion decreased to 0.15, but the maximum gradient distortion increased to 0.08. Table 2 compares total pressure-based diffuser performance parameters for the blowing-on and blowing-off cases. This comparison highlights the difference between the two methods used to calculate distortion. The min/max distortion decreased for the blowing-on case since the minimum total pressure and the face-averaged total pressure measured at the exit plane were both higher than without blowing. The maximum gradient distortion increased with the blowing on, because the local gradients in the total pressure field were larger. The total pressure gradient in the y direction was no longer uniform, and significant total pressure gradients existed in the z direction in the lower half of the duct. The use of VGJs for flow control decreased the energy losses in the diffuser, as evidenced by increased pressure recovery and isentropic efficiency, at the expense of a less uniform total pressure field, evidenced by the increased maximum gradient method distortion.

While total pressure measurements give a useful indication of the way blowing redistributes momentum in the diffuser, they do not lend much understanding of how the redistribution

Table 2 Total pressure-based diffuser performance

Measured quantity	$r_d\|_{av}$	η_d	Min/max	Gradient
Blowing off	0.93	0.69	0.17	0.06
Blowing on	0.94	0.75	0.15	0.08
% change	1.37	8.22	−10.6	49.1

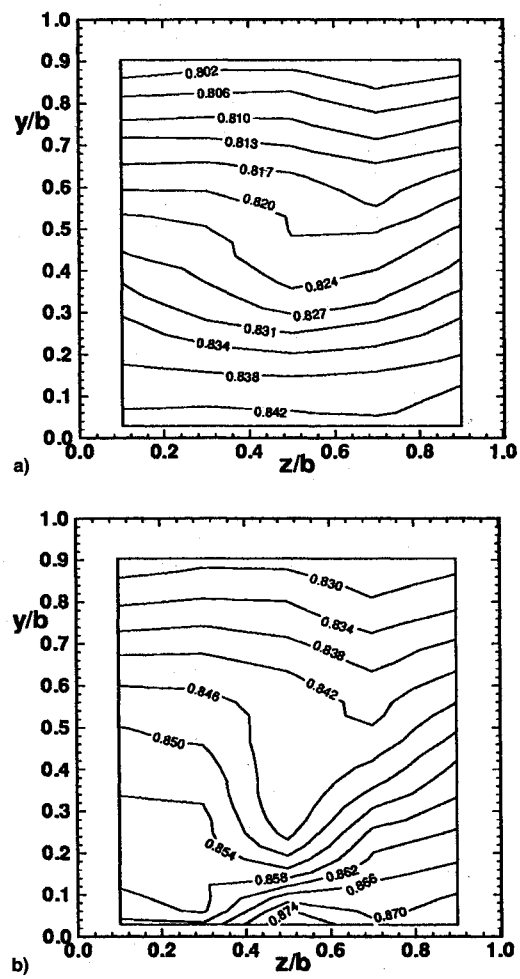

Fig. 5 Exit plane static pressure map: a) blowing off and b) blowing on.

occurs. Obviously, the VGJs do more than just add high-momentum fluid to the flow. The decrease in momentum in the lower left corner of the exit plane is counterintuitive, since the high-momentum fluid from the jets is directed towards that location as it leaves the jet orifices. Other measurements were necessary to attempt to deduce the flow processes occurring in the diffuser with the VGJs blowing.

Static Pressure

The static pressure field was measured across the diffuser exit plane for the blowing-off and $(\dot{m}_j/\dot{m}_d) = 0.0048$ cases. With the blowing off, the static pressure decreased smoothly from its maximum at the lower surface to its minimum value at the upper surface (Fig. 5). The overall face-averaged value of (P_s/P_0) was 0.82. The pressure gradient in the y direction was nearly uniform and there was essentially no pressure gradient in the z direction. The pressure gradient in the y direction resulted from the local acceleration occurring in the upper half of the duct and the local deceleration in the lower half of the duct because of the axial curvature. It drove the secondary flows that caused boundary-layer fluid from all surfaces to migrate toward the surface on the inside of the curve.

Blowing modified the exit plane static pressure field only slightly (Fig. 5). The face-averaged value of static pressure recovery was significantly increased to 0.85, and the magnitude of the pressure difference between the upper and lower surfaces appeared to be nearly the same. Pressure gradients still existed primarily in the y direction, though the gradient was steeper near the lower surface, and local regions of lateral pressure gradient were more prevalent. While the highest value of static pressure was measured near the lower surface centerline, the entire lower corner near the $z/b = 1.0$ sidewall exhibited the greatest overall increases in static pressure recovery over the blowing-off case. This result was consistent with the results from surface flow visualization and total pressure recovery data, which suggested that high-momentum fluid reached the closest to the lower surface between the $z/b = 0.4$ and 1.0 wall. Less energy was lost to the boundary layer, and so more was available for conversion into pressure energy. Because the fluid in the lower right quadrant of the test section had higher momentum than that in the lower left, it experienced a greater compression because of the curvature of the diffuser.

The overall duct C_p increased from 0.24 to 0.38 under the influence of blowing. Thus, blowing, as implemented in this diffuser, increased the static pressure rise achieved in the diffuser by over 50%. This suggests that implementation of a BLC system using vortex generator jets could permit short, highly offset diffusers to achieve the same pressure rise currently obtained by longer or less-offset ducts. The increased distortion of the exit plane static pressure field, like that of the total pressure field, is not a desirable result, and its effects must be considered relative to the gain in pressure recovery.

Mach Number

The peak Mach number with blowing off was near 0.54, while with blowing on this decreased to just below 0.50. This was because of the increased diffusion achieved when the blowing was on. The higher static pressure at the exit plane meant that for an equivalent total pressure the flow Mach number was lower.

Blowing did increase the Mach number in the vicinity of the lower surface. The minimum Mach number measured with blowing on was just above 0.1, compared to 0.0 for blowing off. This is consistent with the observation from total and static pressure data that the near-surface flow maintained some $+x$ momentum with blowing on, while it did not when the blowing was off.

Mean Velocity and Flow Angularity

Cross-wire probes provided information on the three mean velocity components, $\bar{u}$, $\bar{v}$, and $\bar{w}$. The effect of blowing on each of these components is presented in Fig. 6 at three spanwise stations. Again, the increased axial momentum near the lower surface induced by the VGJs is evident.

The local flow angle may be determined from the relative magnitude of the velocity components at a point. This data provided valuable insight into the rotational behavior of the flow.

The spanwise component of mean velocity $\bar{w}$, and hence, the xz-plane flow angle, was strongly affected by the blowing. Without blowing, the spanwise velocity component at either off-centerline station showed that the flow near the lower surface was moving toward the centerline. At some y/b away from the surface, the sign of $\bar{w}$ changed, indicating the point at which the flow was directed away from the centerline. This suggests the existence of a counter-rotating vortex pair imbedded in the flow near the lower surface at the exit plane; a feature also noted by other researchers.[11–14] These vortices are formed by the secondary flows generated in the first bend; they convect fluid along the lower surface toward the centerline before lifting it away from the surface and turning it back outboard. Data obtained along the exit plane centerline clearly show the influence of this counter-rotating pair.

Activation of the VGJs effectively eliminated this structure at the exit plane and replaced it with a pair of vortices of opposite rotation to those that existed with the blowing off. At $z/b = 0.3$, the flow was directed toward the $z/b = 0$ sidewall below $y/b = 0.28$. This was consistent with the results from surface flow visualization. Above $y/b = 0.28$, $\bar{w}$ changed sign and the flow angle pointed toward the center of the diffuser.

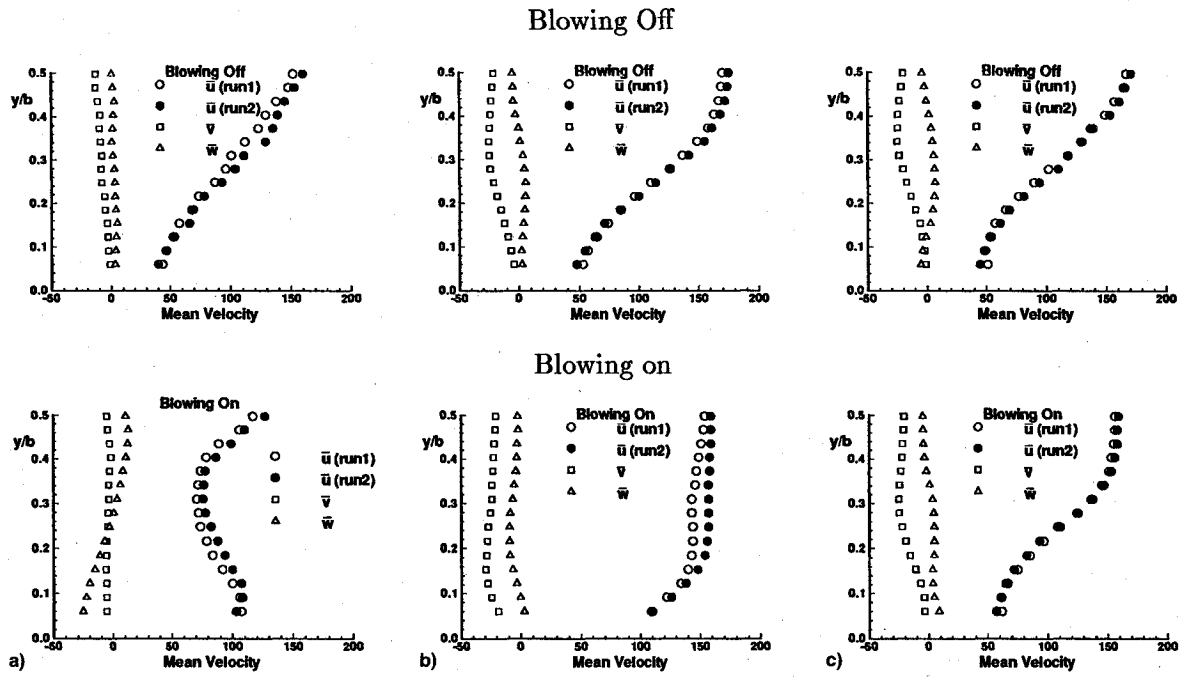

Fig. 6 Mean velocity component profiles. z/b = a) 0.3, b) 0.5, and c) 0.7.

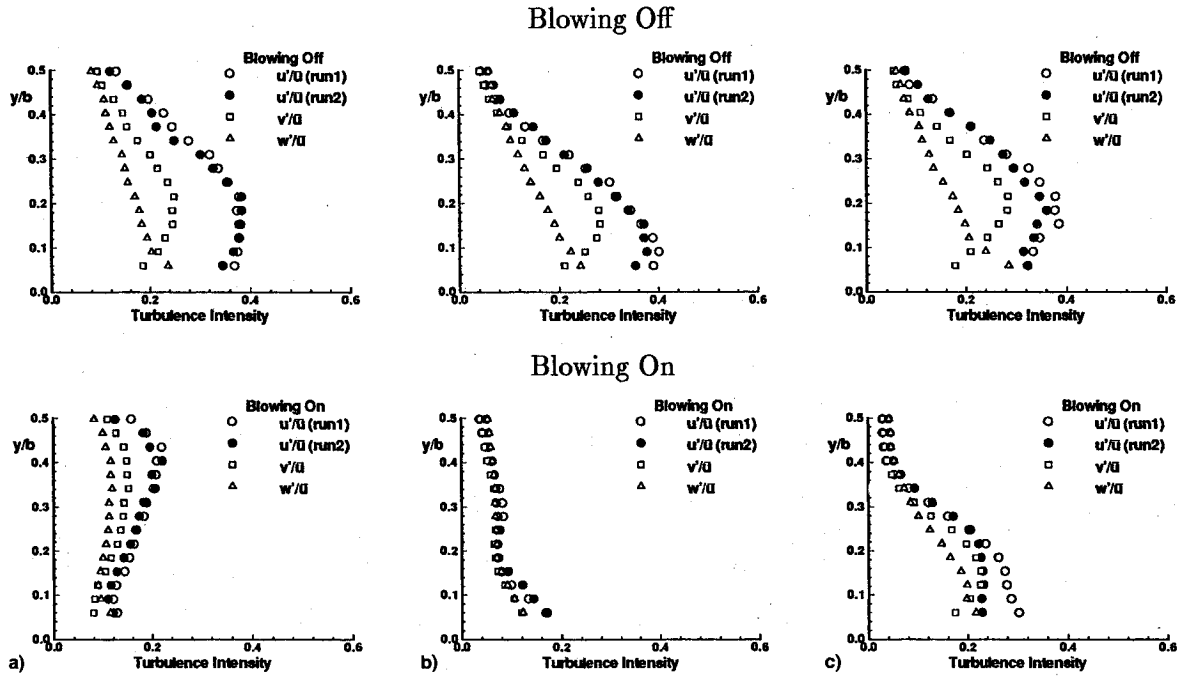

Fig. 7 Turbulence intensity components. z/b = a) 0.3, b) 0.5, and c) 0.7.

At $z/b = 0.7$, the surface flow angle pointed toward the $z/b = 1.0$ sidewall.

While the flow angularity data at the exit plane with the blowing on is not sufficient to conclusively determine the relative orientation of the vortices at that point, it can be construed to support one possible arrangement that is compatible with both the VGJ experience and other behavior observed during this experiment. VGJs generate vortices through entrainment of adjacent fluid,[15] and the vortex on the freestream side of the canted jet becomes dominant. In this installation, the jets were canted toward the $z/b = 0$ sidewall, and the dominant vortex would then rotate clockwise. Formation of such a structure inside the test diffuser would tend to sweep low-momentum fluid from the lower surface toward the $z/b = 0$ sidewall, and then lift it up along that sidewall. This would then account for deflection of the lower surface streaklines toward the $z/b = 0$ corner as observed during flow visualization, and for the low-momentum region measured along that wall seen in the pitot–static data.

Turbulence Intensity

Figure 7 depicts the three components of turbulence intensity measured at the centerline station ($z/b = 0.5$) cross-film probes with and without blowing. The local mean velocity component $\bar{u}$ is used as the nondimensionalizing parameter. Note that though the u' component was largest, the v' and w' were significant. At its maximum, u' was equal to nearly 40% of the mean component $\bar{u}$.

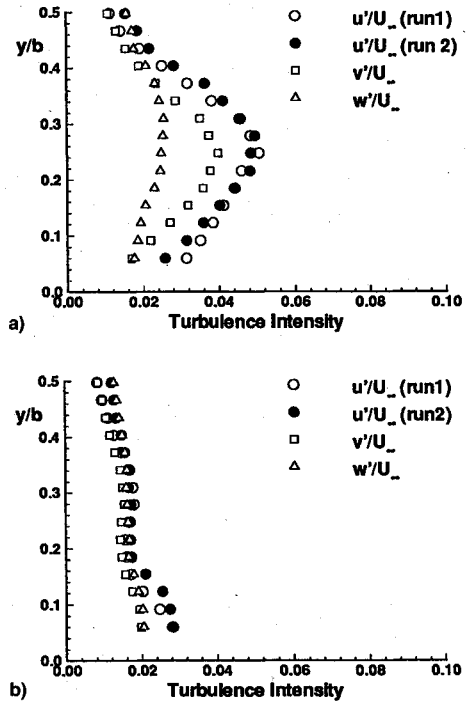

Fig. 8 Turbulence intensity components, nondimensionalized by U_∞, blowing off (z/b = 0.5): a) blowing off and b) blowing on.

Also presented in Fig. 7 are the turbulence intensity profiles measured for $(\dot{m}_j/\dot{m}_d)$ = 0.0048. Blowing reduced the maximum values for each component of turbulence intensity, and the shape of the turbulence intensity profiles varied with spanwise position. At z/b = 0.3, maximum values for turbulence intensity were measured around y/b = 0.4, far above the lower surface, but in the region of low-momentum fluid documented in the mean flow analysis. The maximum value of u' was about 25% of $\bar{u}$. At the centerline, where the boundary-layer profile was the fullest, all components of turbulence intensity were nearly equal. The maximum value was less than 0.20. At z/b = 0.7, the turbulence profile looked similar to that observed in the absence of blowing, but the peak magnitude of u' was reduced to 30% of $\bar{u}$.

Part of the apparent reduction in turbulence intensity with the blowing on was because of the increased mean velocity at that condition. The local mean velocity was chosen as the nondimensionalizing quantity so that turbulence intensity would be a measure of the magnitude of the local fluctuation velocity component relative to the local mean velocity component. While this is useful, $\bar{u}$ changes across the boundary layer, making it difficult to determine the behavior of the fluctuating components themselves. Turbulence intensity can also be nondimensionalized by some reference velocity; the freestream velocity is commonly used.

For comparison, Fig. 8 shows the turbulence intensity nondimensionalized by the inlet plane freestream velocity at z/b = 0.5, with the blowing off and on. These figures show one significant feature that was misrepresented by the initial choice of a nondimensionalizing quantity, the maximum value of w' occurred at the same vertical position as the maximum for u' and v' rather than adjacent to the lower surface as the previous normalization indicated. The maximum values were measured almost exactly at the midpoint of the boundary layer. Each fluctuation component dropped off rapidly towards the wall. The blowing-on profile did not change significantly when nondimensionalized in this way. Turbulence intensity was still significantly reduced over the blowing-off case.

Turbulent Kinetic Energy

Turbulent kinetic energy is a measure of the kinetic energy of the turbulent fluctuations; it represents energy that is lost from the mean flow. When nondimensionalized by $\bar{u}^2$, it represents the ratio of the kinetic energy in the local turbulent motion to the kinetic energy of the local downstream mean motion. Figure 9 shows profiles of turbulent kinetic energy computed from the measured fluctuation velocity components at z/b = 0.5, with the blowing on and off. At the edge of the boundary layer, where the fluctuation velocities are small, the energy drained by the turbulence is less than 1% of that held in the flow. With the blowing off, this value increased as the lower surface was approached. It reached a maximum of 12–14% of the directed energy around y/b = 0.15, then decreased as the fluctuations diminish near the wall. Like the turbulence intensity profiles, the turbulent kinetic energy profiles with the blowing off were relatively independent of spanwise location.

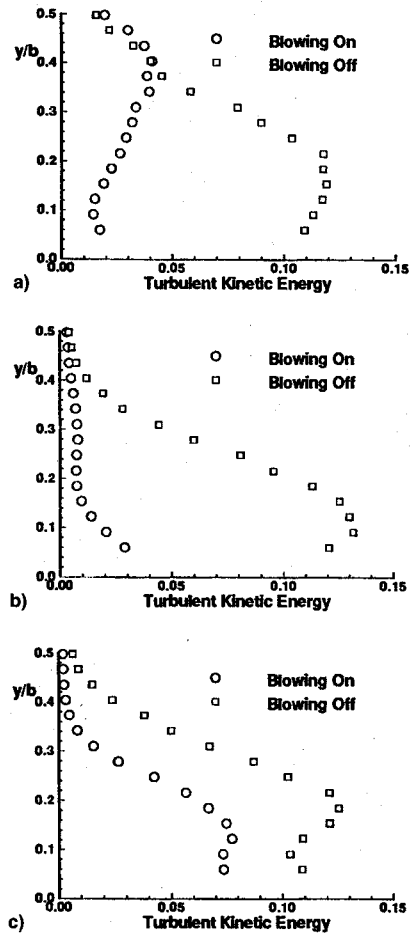

Fig. 9 Effect of blowing on turbulent kinetic energy. z/b = a) 0.3, b) 0.5, and c) 0.7.

With the blowing on, the turbulent kinetic energy became more dependent upon a spanwise position. At z/b = 0.3, turbulent kinetic energy was at its maximum relative to the local mean velocity in the low-momentum region above the jet plume. At stations nearer the wall, the turbulent kinetic energy was 8% less than for the blowing off case. At z/b = 0.5, the freestream level of turbulent kinetic energy was retained much closer to the wall than for the blowing-off case, and the maximum value measured was 3% of the local mean flow kinetic energy, as opposed to 13% without blowing. At z/b = 0.7, the blowing-on turbulent kinetic energy profile was similar to that measured with the blowing off, though the value of the turbulent kinetic energy was typically 6–8% less.

Conclusions

A detailed experimental study of the use of VGJs in a highly offset diffuser was performed for an inlet Mach number of 0.6 and an $Re_{eq} = 3.46 \times 10^7$.

Without blowing, the lower surface boundary layer was massively separated over most of the length of the diffusing section. Diffuser performance, as characterized by total pressure recovery and a static pressure coefficient, suffered as a result. A significant amount of energy was lost to turbulence. This conclusion was substantiated by observations from surface flow visualization and from measured static pressure, total pressure, and turbulence data. A strong local adverse pressure gradient and strong secondary flows produced by the curvature of the diffuser surfaces combined to create conditions favorable for flow separation along the lower surface of the diffuser. The lower-surface boundary layer occupied nearly half of the duct cross section at the exit plane.

The use of blowing vortex generator jets for BLC on the lower surface of the diffuser resulted in improved overall performance with a blowing mass flow rate equal to 0.48% of the diffuser inlet mass flow rate. The static pressure coefficient increased 50% from the value measured without blowing, while face-averaged pressure recovery increased 1.3% and the diffuser isentropic efficiency increased as well. The extent of the separated flow region on the lower surface decreased, and the surface flow patterns were altered so that most reverse flow was eliminated. The exit plane boundary-layer thickness was reduced at most locations, particularly near the centerline.

With the vortex generator jets operating, low-momentum fluid accumulated near the sidewall towards which the jets were canted. The momentum of the fluid on the other side of the diffuser was increased over measurements taken without blowing. This redistribution of the flow momentum resulted in increased distortion of the total pressure and static pressure fields at the exit plane.

The level of turbulence present in the flow at the exit plane was reduced when the vortex generator jets were operating, particularly near the centerline. The magnitude of the turbulent velocity fluctuation components was reduced, resulting in less energy being transferred from the mean flow to the turbulent motion. A reduction in the turbulent kinetic energy accounted for some of the increase in efficiency realized when the vortex generator jets were operating.

Use of vortex generator jets greatly altered the structure of both the primary and secondary flows within the diffuser. The streamwise momentum distribution was altered, and the direction of rotation of the secondary flows was reversed at the exit plane. The mechanism by which the VGJs accomplished those changes was not determined.

References

[1]Adkins, R., "Diffusers and Their Performance Improvement by Means of Boundary Layer Control," AGARD-R-754, 1977.

[2]Ball, W., "Tests of Wall Blowing Concepts for Diffuser Boundary Layer Control," AIAA Paper 84-1276, June 1984.

[3]Wallis, R., "The Use of Air Jets for Boundary Layer Control," Aerodynamics Research Labs., Note 110, Australia, 1952.

[4]Johnston, J., and Nishi, M., "Vortex Generator Jets—A Means for Passive and Active Control of Boundary Layer Separation," AIAA Paper 89-0564, Jan. 1989.

[5]Selby, G., Lin, J., and Howard, F., "Control of Low-Speed Turbulent Separated Flow Using Jet Vortex Generators," *Experiments in Fluids*, Vol. 12, No. 6, 1992, pp. 394–400.

[6]Lin, J., Howard, F., Bushnell, D., and Selby, G., "Investigation of Several Passive and Active Methods for Turbulent Flow Separation Control," AIAA Paper 90-1598, June 1990.

[7]Ball, W., "Experimental Investigation of the Effects of Wall Suction and Blowing on the Performance of Highly Offset Diffusers," AIAA Paper 83-1169, June 1983.

[8]Lee, C., and Price, W., "Subsonic Diffusers for Highly Survivable Aircraft," Air Force Wright Aeronautical Labs.-TR-86-3025, June 1986.

[9]Senseney, M., "Performance Characterization of a Highly Offset Diffuser with and Without Vortex Generator Jets," M.S. Thesis, U.S. Air Force Inst. of Technology, Wright–Patterson AFB, OH, 1994.

[10]Hill, P., and Peterson, C., *Mechanics and Thermodynamics of Propulsion*, Addison–Wesley, Reading, MA, 1992.

[11]Vakili, A., Wu, J., Hingst, W., and Towne, C., "Comparison of Experimental and Computational Compressible Flow in an S-Duct," AIAA Paper 84-0033, Jan. 1984.

[12]Bansod, P., and Bradshaw, P., "The Flow in S-Shaped Ducts," *Aeronautical Quarterly*, Vol. 23, No. 2, 1972, pp. 131–140.

[13]Wellborn, S., Rechert, B., and Okiishi, T., "An Experimental Investigation of the Flow in a Diffusing S-Duct," AIAA Paper 92-3622, July 1992.

[14]Tindell, R., "Highly Compact Inlet Diffuser Technology," AIAA Paper 87-1747, July 1987.

[15]Zhang, X., and Collins, M., "Flow and Heat Transfer in a Turbulent Boundary Layer Through Skewed and Pitched Jets," *AIAA Journal*, Vol. 31, No. 9, 1993, pp. 1590–1598.